Tetrahedron Letters 49 (2008) 7200–7203

Contents lists available at ScienceDirect

Tetrahedron Letters

journal homepage: www.elsevier.com/locate/tetlet

# Synthesis, structure, and photoelectrochemical properties of new tetrathiafulvalene-diphenyl-1,3,4-oxadiazole dyads

Hideki Fujiwara *, Yasuo Sugishima, Keijiro Tsujimoto

*Department of Chemistry, Graduate School of Science, Osaka Prefecture University, Gakuen-cho, Sakai 599-8570, Japan*

ARTICLE INFO

*Article history:*
Received 28 August 2008
Revised 29 September 2008
Accepted 1 October 2008
Available online 2 October 2008

ABSTRACT

New donor–acceptor dyads containing tetrathiafulvalene (TTF) and 2,5-diphenyl-1,3,4-oxadiazole (PPD) moieties were synthesized to develop new photoconducting materials. Crystal structure analysis indicated the highly planar molecular skeleton of the dyad. Fluorescence from the PPD part was almost quenched by the intramolecular electron transfer from the TTF part to the PPD part. Photoelectrochemical measurements indicate that cathodic photocurrents can be generated from a thin film of the dyad spin-coated on ITO electrode.

Recently, donor–acceptor type dyads using a tetrathiafulvalene (TTF) framework have received considerable interest as materials for fluorescence switches, chemical sensors, molecular rectification, and photovoltaic and NLO applications.[1–6] The photo-induced interactions between the donor and acceptor parts such as intramolecular charge-transfer interactions and the resultant formation of charge-separated state have played an important role for the development of optoelectronic devices.[7,8] We focused on the development of photo-induced conducting materials based on the organic conductors in which their conductivities can be switched by external lights. 2,5-Diphenyl-1,3,4-oxadiazole (PPD) and its derivatives are known to show strong fluorescence, and are used as electron-transport materials in electroluminescence devices.[9,10] We designed new donor–acceptor dyads containing TTF and PPD moieties (**1**) to realize novel photo-switchable conducting materials. In this Letter, we report the synthesis, structure and photoelectrochemical properties of **1a**, **b**.

Synthesis of **1a**, **b** was performed as described in Scheme 1. Thus, tributylstannyl-substituted TTF (**2**) was prepared from TTF by the reported method.[11] Then, Pd($PPh_3$)$_4$-catalyzed Stille coupling reaction of **2** and bromo-substituted PPD derivatives (**3a**, **b**)[12,13] was performed under toluene reflux for 24 h. After column chromatography on silica gel with $CHCl_3$ as an eluent, compounds **1a**, **b** were obtained as red microcrystals in 37% and 53% yields, respectively.[14] The cyclic voltammograms of **1a**, **b** were measured in benzonitrile at 25 °C. Compound **1** showed two pairs of one-electron reversible redox waves as summarized in Table 1. Because these redox potentials are almost similar to those of TTF ($E_1$ = +0.41 V and $E_2$ = +0.80 V under the identical condition), compounds **1a**, **b** have a good electron-donating ability despite the substitution of the electron-withdrawing 1,3,4-oxadiazole ring.

In the UV–vis absorption spectra measured in $10^{-4}$ M $CHCl_3$ solution at room temperature, **1a** showed a strong absorption maximum at 312 nm (log ε = 4.55) and a weak maximum at 453 nm

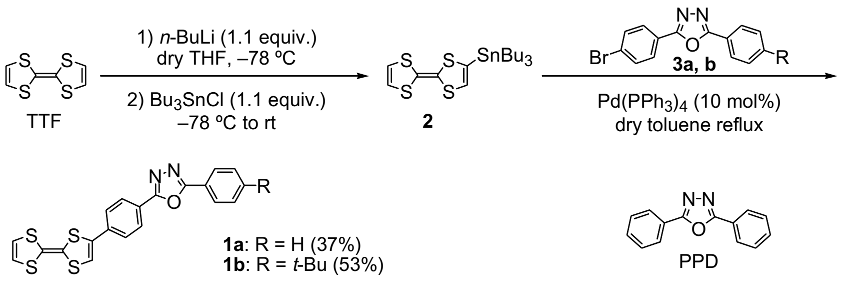

**Scheme 1.** Synthesis of **1a** and **1b**.

---

* Corresponding author. Tel.: +81 72 254 9818; fax: +81 72 254 9935.
*E-mail address:* hfuji@c.s.osakafu-u.ac.jp (H. Fujiwara).

0040-4039/$ - see front matter © 2008 Elsevier Ltd. All rights reserved.
doi:10.1016/j.tetlet.2008.10.001

**Table 1**
Redox potentials of **1a**, **b** and TTF[a]

| Compound | $E_1$/V | $E_2$/V | $E_2 - E_1$/V |
|---|---|---|---|
| **1a** | +0.43 | +0.83 | 0.40 |
| **1b** | +0.44 | +0.84 | 0.40 |
| TTF | +0.41 | +0.80 | 0.39 |

[a] $V$ versus Ag/AgCl, 0.1 mol $L^{-1}$ $n$-$Bu_4NClO_4$ in benzonitrile at 25 °C, Pt electrodes, scan rate of 50 mV $s^{-1}$.

(log $\varepsilon$ = 3.65), whereas absorption maxima were observed at 312 and 369 nm in the case of TTF, as shown in Figure 1. PPD also showed a strong maximum at 282 nm (log $\varepsilon$ = 4.43). Molecular orbital (MO) calculation of **1a** was performed by the density functional theory, B3LYP/6-31G** method using GAUSSIAN 93. As shown in Figure 2, the atomic coefficients of HOMO and LUMO orbitals of **1a** are mainly localized on the TTF and PPD moieties, respectively. The energy of HOMO–LUMO gap is estimated to be 2.65 eV (=1240/2.65 = 468 nm) from the energy levels of HOMO (−4.72 eV) and LUMO (−2.07 eV), and is almost equal to the weak absorption maximum at 453 nm of **1a**, suggesting that this absorption corresponds to the charge-transfer absorption from TTF part to PPD part. On the other hand, the MO calculation also suggests that the excitations within each TTF or PPD part occur at 3.68 eV (=337 nm; HOMO to LUMO+2) and 4.00 eV (=310 nm; HOMO−1 to LUMO), respectively. These excitations may correspond to the strong and broad maximum around 312 nm of **1a**.

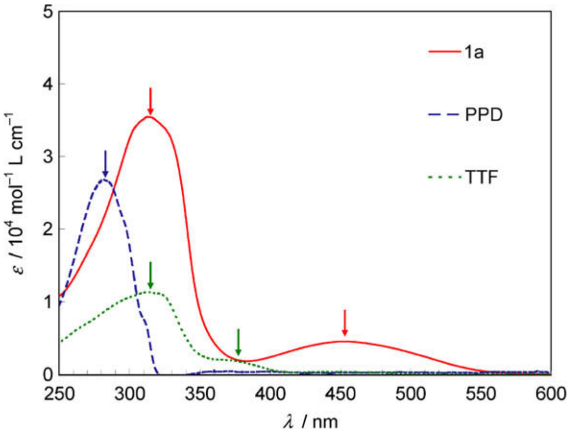

**Figure 1.** UV–vis absorption spectra of **1a**, PPD, and TTF in $10^{-4}$ M $CHCl_3$ solution. Arrows indicate absorption maxima.

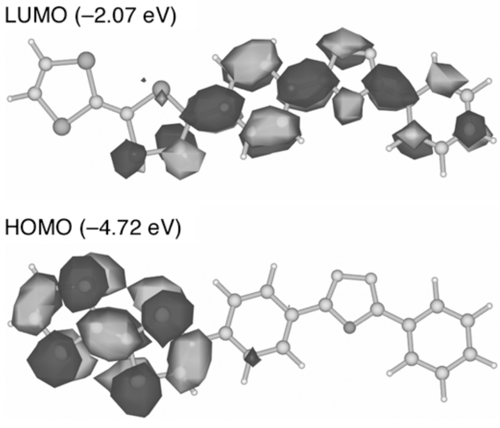

**Figure 2.** LUMO and HOMO orbitals of **1a** calculated by B3LYP/6-31G** method.

An X-ray crystal structure analysis of **1a** was performed using a red plate-like single crystal of **1a** recrystallized from $CHCl_3$/methanol.[15] In the unit cell, there are two crystallographically independent molecules A and B. As shown in Figure 3, both of them have almost planar molecular skeletons, and adopt only one of two possible planar conformers. As Figure 4 indicates molecule **1a** constructs –B–A–A′–B′-type stackings along the $a$-axis. Donor molecules B form a dimer (B–B′) with overlapping its PPD part over the TTF part, whereas only PPD parts are overlapped to each other in the dimer of A–A′. In the A–B overlap, each TTF part and PPD part stack to each other in a head-to-head overlap mode. Because of such a mixed-stacking structure of the TTF and PPD parts, it is considered to be difficult to realize photo-induced conductivities using this single crystal. However, the high planarity of this molecular framework will be favorable to construct effective conducting pathways if appropriate derivatives having substituents adequate for the construction of segregated stacking structures of TTF and PPD moieties can be utilized.

Emission spectra of **1**, PPD, and TTF were measured in $10^{-4}$ M $CHCl_3$ solutions at room temperature. When the solution of PPD was irradiated by the excitation light of 282 nm that corresponds to the absorption maximum of PPD, already-known quite strong fluorescence was observed around 350 nm. However, in the case of the $CHCl_3$ solution of **1a** and **1b**, only a subtle fluorescence that may correspond to the fluorescence of TTF part was observed around 375 nm (Fig. 6). This result suggests that the fluorescence from the excited PPD (PPD*) part is almost quenched by the intramolecular electron-transfer process from the electron-donating TTF part to the PPD* part because the PPD* part possesses electron-accepting ability upon excitation.[16–18] To examine the fluorescence quenching by the electron transfer process, UV–vis absorption spectra and emission spectra of **1b** were measured on various oxidation states of **1b** as shown in Figures 5 and 6, respectively. Upon step-wise addition of an oxidation reagent ($NOBF_4$) to the $CHCl_3$ solution of **1b**, the color of the solution changed from orange to green with an absorption increase around 630 nm, then to light yellow with weak shoulder absorption over 400 nm. These color changes correspond to the oxidation processes from **1b** to $\mathbf{1b}^{+\cdot}$ and to $\mathbf{1b}^{2+}$ states. Such a clear color change upon oxidation was also reported in the other TTF derivatives bearing a PPD part through ethynyl-spacer, which can be used as electrochromic materials.[19] As shown in Figure 6, upon oxidation to $\mathbf{1b}^{+\cdot}$ state, the emission intensity around 375 nm was almost unchanged. On the other hand, further oxidation process to $\mathbf{1b}^{2+}$ state largely increases the emission intensity around 390 nm. These results indicate that the addition of excess $NOBF_4$ oxidizes the TTF part to its dication state $TTF^{2+}$, and suppresses the electron-donating ability of TTF part that can quench the emission from the PPD* part, and allows the emission from the PPD* part.[20–22] Such a combination of multi-redox property of the TTF moiety and fluorescence ability of the PPD part may be used as fluorescence switches and chemical sensors.[23–26]

As mentioned above, photo-induced intramolecular electron-transfer process quenches the emission from PPD*. During this process, photo-induced charge-transfer state $TTF^{+\cdot}$–$PPD^{-\cdot}$ can be achieved. To examine the possibility of photo-induced electric current generation from such a charge-transfer excited state, measurement of photocurrents was performed by photoelectrochemical method. Thin film of **1a** was deposited on an ITO-coated soda-lime glass substrate (Aldrich No. 576352; 1.6 cm × 1.6 cm) by spin-coating using 5 μL of 1 g $L^{-1}$ solution of **1a** in $CHCl_3$ at 2000 rpm for 30 s. These conditions for the preparation of thin films are optimized by repeating photoconductivity measurements with changing the volume and concentration of solution, speed and time of spinning. Photoelectrochemical measurements using this thin film-coated ITO electrode (spin-coated area: 1.0 cm × 0.8 cm)

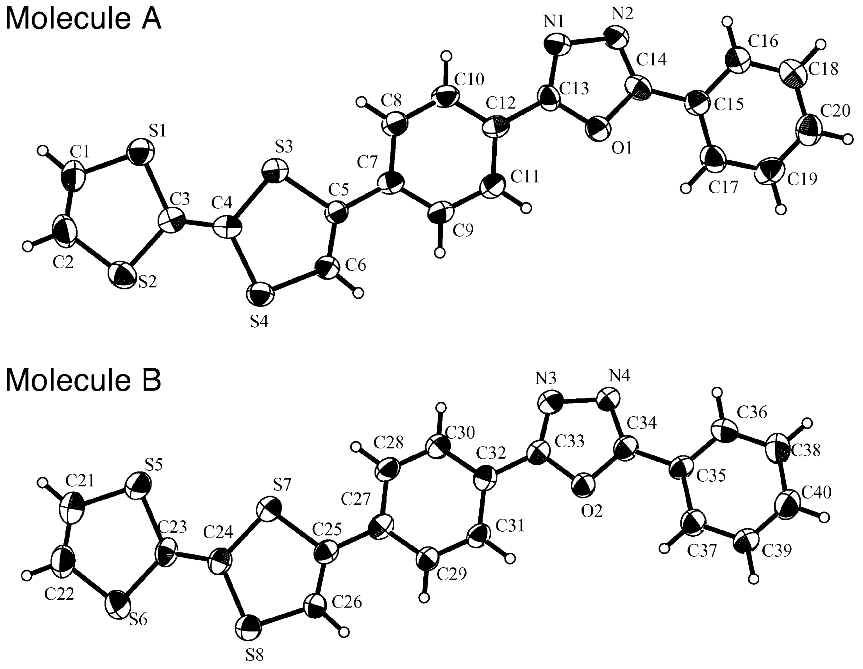

**Figure 3.** Molecular structures of molecules A and B of **1a**.

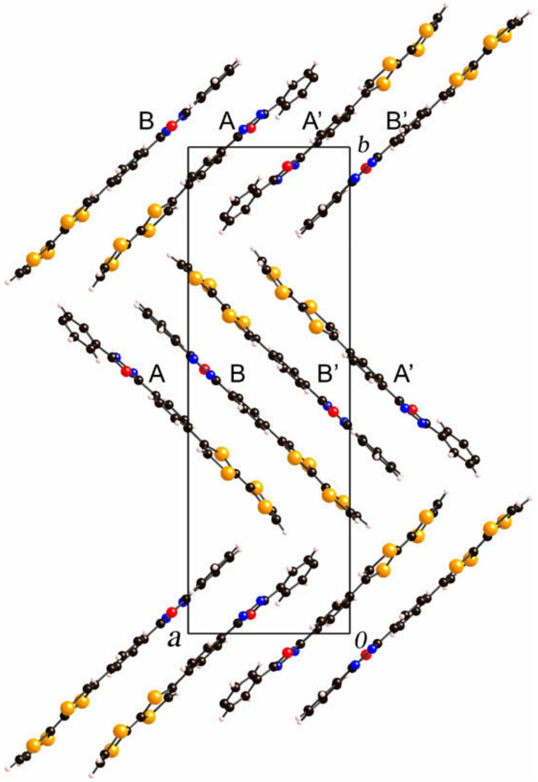

**Figure 4.** Crystal structures of **1a** projected on to the *ab*-plane.

as working electrode were performed in 0.1 mol L$^{-1}$ aqueous KCl solution.[27] Platinum and Ag/AgCl electrodes were used as counter and reference electrodes, respectively. Photocurrents between the working and counter electrodes were measured by BAS Electrochemical Analyzer Model 612B under irradiation from 150 W Xe lamp, where monochromatized light in the wavelength range from 300 to 600 nm was produced by holographic monochromators

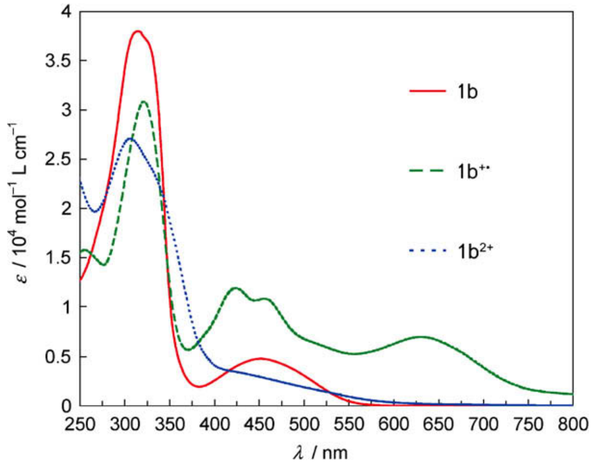

**Figure 5.** UV–vis absorption spectra of **1b**, **1b**$^{+\cdot}$, and **1b**$^{2+}$ in 10$^{-4}$ M $CHCl_3$ solution upon oxidation of **1b** by $NOBF_4$.

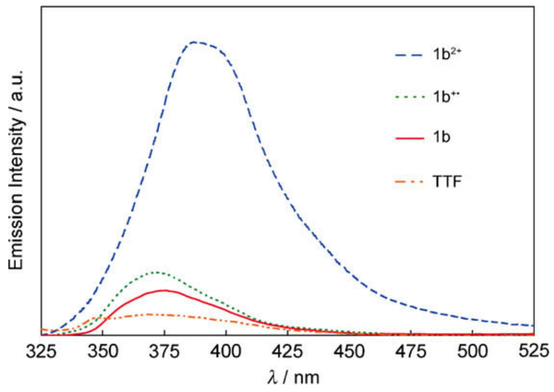

**Figure 6.** Emission spectra of **1b**, **1b**$^{+\cdot}$, **1b**$^{2+}$, and TTF in 10$^{-4}$ M $CHCl_3$ solution upon oxidation of **1b** by $NOBF_4$ (excitation light of 315 nm).

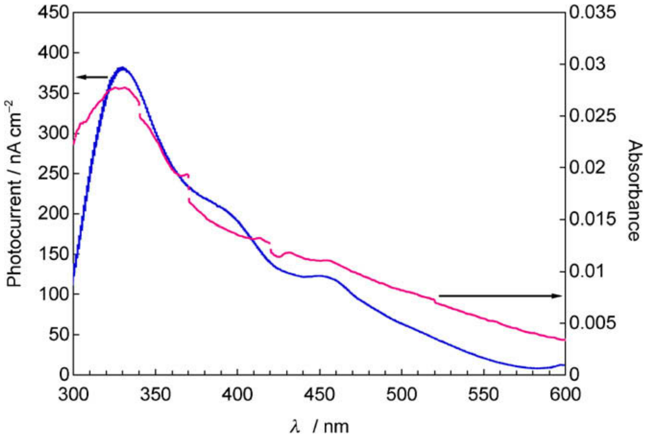

**Figure 7.** Photocurrent action spectrum under zero bias voltage versus Ag/AgCl reference electrode and absorption spectrum of the thin film of **1a** spin-coated on ITO electrode.

using fluorescence spectrometer JASCO FP-6200. The photocurrent action spectrum for the thin film of **1a** on ITO electrode was measured under zero bias voltage versus Ag/AgCl reference electrode. As shown in Figure 7, a broad cathodic photocurrent maximum of $I_{\max} = 390$ nA/cm$^2$ was observed for **1a** around 330 nm, which corresponds to the absorption maximum of the identical thin film of **1a** on ITO electrode, suggesting that the absorbed photons were converted to electric currents. The conversion yield of photo-electric conversion ($\eta$) was calculated to be 0.26% at 330 nm from $I_{\max}$, absorbance of thin film (0.027), and the power of irradiated light (8.9 mW/cm$^2$).[27,28] This conversion yield of 0.26% is almost the same order of the reported ones using the LB films of D–π–A type dyads (0.40%) and $D_2M(dmit)_2$ complexes (1.1%).[27,28] Such a cathodic photocurrent indicates that when molecule **1a** is irradiated to the excited state **1a***, the excited electron flows to the electrolyte solution, then the electron transfers from the conduction band of ITO electrode (–4.5 V)[29] to the hole generated on molecule **1a**. Since only small or zero photocurrents were observed in the cases of thin films of TTF or PPD, large cathodic photocurrents that were observed in the case of **1a** can be regarded as the result of charge-transfer process between the TTF and PPD parts. Figure 8 shows the bias voltage (vs Ag/AgCl) dependence of photocurrents of thin film of **1a** spin-coated on ITO electrode under irradiation light of 330 nm using another thin film of **1a** that is different from the one used for the measurement of Figure 7. The cathodic photocurrents increase with increasing negative bias voltage, suggesting that such a negative bias voltage promotes the electron-transfer process on the **1a**-modified ITO electrode. The conversion yield of photo-electric conversion ($\eta$) reached to about 1.6% under the bias voltage of −0.4 V versus Ag/AgCl reference electrode.

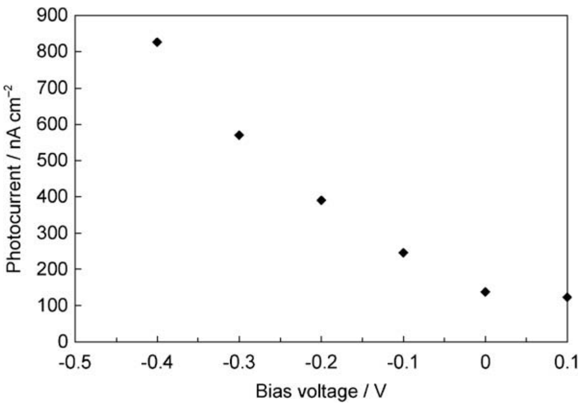

**Figure 8.** Bias voltage (vs Ag/AgCl) dependence of photocurrents of the thin film of **1a** spin-coated on ITO electrode under irradiation light of 330 nm.

In conclusion, we have synthesized new donor–acceptor type TTF dyads in which TTF part connects directly to a PPD part. The studies on emission spectra suggest the photo-induced intramolecular electron transfer between TTF and PPD parts. The photoelectrochemical measurements indicate that cathodic photocurrents can be generated from the thin film of **1a** that is spin-coated on ITO electrode. These results suggest that the synthesized dyads can be considered as candidates for optoelectronic materials such as photoconducting applications.

## Acknowledgments

This work was financially supported in part by Grants-in-Aid for Scientific Research (Nos. 18028020 and 19750119) from the Ministry of Education, Culture, Sports, Science and Technology of Japan.

## References and notes

1. *TTF Chemistry: Fundamentals and Applications of Tetrathiafulvalene*; Yamada, J., Sugimoto, T., Eds.; Kodansha-Springer: Tokyo, 2004.
2. Martín, N.; Sánchez, L.; Illescas, B.; Pérez, I. *Chem. Rev.* **1998**, *98*, 2527–2547.
3. Metzger, R. M. *Acc. Chem. Res.* **1999**, *32*, 950–957.
4. Bendikov, M.; Wudl, F.; Perepichka, D. F. *Chem. Rev.* **2004**, *104*, 4891–4945.
5. Gorgues, A.; Hudhomme, P.; Sallé, M. *Chem. Rev.* **2004**, *104*, 5151–5184.
6. Segura, J. L.; Martín, N. *Angew. Chem., Int Ed.* **2001**, *40*, 1372–1409.
7. Bryce, M. R. *Adv. Mater.* **1999**, *11*, 11–23.
8. Nishikawa, H.; Kojima, S.; Kodama, T.; Ikemoto, I.; Suzuki, S.; Kikuchi, K.; Fujitsuka, M.; Luo, H.; Araki, Y.; Ito, O. *J. Phys. Chem. A* **2004**, *108*, 1881–1890.
9. Mitschke, U.; Bäuerle, P. *J. Mater. Chem.* **2000**, *10*, 1471–1507.
10. Hughes, G.; Bryce, M. R. *J. Mater. Chem.* **2005**, *15*, 94–107.
11. Iyoda, M.; Kuwatani, Y.; Ueno, N.; Oda, M. *J. Chem. Soc., Chem. Commun.* **1992**, 158–159; Moore, A. J.; Batsanov, A. S.; Bryce, M. R.; Howard, J. A. K.; Khodorkovsky, V.; Shapiro, L.; Shames, A. *Eur. J. Org. Chem.* **2001**, 73–78.
12. Wang, C.; Pålsson, L.-O.; Batsanov, A. S.; Bryce, M. R. *J. Am. Chem. Soc.* **2006**, *128*, 3789–3799.
13. Cha, S. W.; Choi, S.-H.; Kim, K.; Jin, J.-I. *J. Mater. Chem.* **2003**, *13*, 1900–1904.
14. Compound **1a**: mp 238–239 °C (dec.); $^1$H NMR (300 MHz; $CDCl_3$) $\delta$ 8.17–8.12 (m, 4H), 7.57–7.55 (m, 5H), 6.72 (s, 1H), 6.36 (s, 2H); Calcd for $C_{20}H_{12}N_2OS_4$: C, 56.58; H, 2.85; N, 6.60. Found: C, 56.18; H, 2.76; N, 6.44; *m*/*z* 424 [M$^+$, 100%], 425 [M$^+$+1, 35%], 426 [M$^+$+2, 25%]. Compound **1b**: mp 230–232 °C (dec.); $^1$H NMR (300 MHz; $CDCl_3$) $\delta$ 8.14–8.05 (m, 4H), 7.57–7.54 (m, 4H), 6.71 (s, 1H), 6.36 (s, 2H), 1.38 (s, 9H); Calcd for $C_{24}H_{20}N_2OS_4$: C, 59.97; H, 4.19; N, 5.83. Found: C, 59.82; H, 4.04; N, 5.82; *m*/*z* 480 [M$^+$, 100%], 481 [M$^+$+1, 47%], 482 [M$^+$+2, 29%].
15. *Crystal data for* **1a**: $C_{40}H_{24}N_4O_2S_8$, $M = 849.14$, monoclinic, $P2_1/c$, $a = 10.2927(12)$, $b = 29.580(3)$, $c = 12.9844(15)$ Å, $\beta = 107.743(3)°$, $V = 3765.2(7)$ Å$^3$, $Z = 4$, $T = 296$ K, $D_{\text{calc}} = 1.498$ g cm$^{-3}$, $\mu$(Mo K$\alpha$) = 5.18 cm$^{-1}$, Mo K$\alpha$ radiation ($\lambda = 0.71075$ Å), $R_1 = 0.055$, $wR_2 = 0.068$. Crystallographic data (excluding structure factors) of this crystal have been deposited with the Cambridge Crystallographic Data Centre as supplementary publication No. CCDC-699798. Copies of the data can be obtained, free of charge, on application to CCDC, 12 Union Road, Cambridge CB2 1EZ, UK, [fax: +44-(0)1223-336033 or e-mail: deposit@ccdc.cam.ac.uk].
16. Farren, C.; Christensen, C. A.; FitzGerald, S.; Bryce, M. R.; Beeby, A. *J. Org. Chem.* **2002**, *67*, 9130–9139.
17. Wang, C.; Bryce, M. R.; Batsanov, A. S.; Stanley, C. F.; Beeby, A.; Howard, J. A. K. *J. Chem. Soc., Perkin Trans. 2* **1997**, 1671–1678.
18. Loosli, C.; Jia, C.; Liu, S.-X.; Haas, M.; Dias, M.; Levillain, E.; Neels, A.; Labat, G.; Hauser, A.; Decurtis, S. *J. Org. Chem.* **2005**, *70*, 4988–4992.
19. Wang, C.; Batsanov, A. S.; Bryce, M. R. *Chem. Commun.* **2004**, 578–579.
20. Leroy-Lhez, S.; Baffreau, J.; Perrin, L.; Levillain, E.; Allain, M.; Blesa, M.-J.; Hudhomme, P. *J. Org. Chem.* **2005**, *70*, 6313–6320.
21. Li, H.; Jeppensen, J. O.; Levillain, E.; Becher, J. *Chem. Commun.* **2003**, 846–847.
22. Sadaike, S.; Takimiya, K.; Aso, Y.; Otsubo, T. *Tetrahedron Lett.* **2003**, *44*, 161–165.
23. Zhang, G.; Zhang, D.; Guo, X.; Zhu, D. *Org. Lett.* **2004**, *6*, 1209–1212.
24. Li, X.; Zhang, G.; Ma, H.; Zhang, D.; Li, J.; Zhu, D. *J. Am. Chem. Soc.* **2004**, *126*, 11543–11548.
25. Xiao, X.; Xu, W.; Zhang, D.; Xu, H.; Lu, H.; Zhu, D. *J. Mater. Chem.* **2005**, *15*, 2557–2561.
26. Fang, C.-J.; Zhu, Z.; Sun, W.; Xu, C.-H.; Yan, C.-H. *New J. Chem.* **2007**, *31*, 580–586.
27. Zhai, J.; Wei, T.-X.; Huang, C.-H.; Cao, H. *J. Mater. Chem.* **2000**, *10*, 625–630.
28. Li, F.-Y.; Jin, L.-P.; Huang, Y.-Y.; Huang, C.-H.; Zheng, J.; Guo, J.-Q. *J. Mater. Chem.* **2001**, *11*, 1783–1788.
29. Thompson, W. G.; Anderson, R. L. *Solid State Electron.* **1978**, *21*, 603–608.